Measurement of glucose exclusion from the fully hydrated DOPE inverse hexagonal phase†

Ben Kent,[a] Christopher J. Garvey,[b] Thomas Lenné,[c] Lionel Porcar,[de] Vasil M. Garamus[f] and Gary Bryant*[a]

Received 22nd September 2009, Accepted 22nd December 2009
First published as an Advance Article on the web 19th January 2010
DOI: 10.1039/b919086d

The degree of exclusion of glucose from the inverse hexagonal H_{II} phase of fully hydrated DOPE is determined using contrast variation small angle neutron scattering and small angle X-ray scattering. The presence of glucose is found to favour the formation of the non-lamellar H_{II} phase over the fluid lamellar phase, over a wide range of temperatures, while having no significant effect on the structure of the H_{II} phase. Glucose is preferentially excluded from the lipid–water interface resulting in a glucose concentration in the H_{II} phase of less than half that in the coexisting aqueous phase. The degree of exclusion is quantified and the results are consistent with a hydration layer of pure water adjacent to the lipid head groups from which glucose is excluded. The osmotic gradient created by the difference in glucose concentration is determined and the influence of glucose on the phase behaviour of non-lamellar phase forming lipid systems is discussed.

Introduction

Dehydration of biological tissue can induce phase transitions in cellular lipid membranes that affect the ability of the membrane to act as a semi-permeable barrier and are a pathway to irreversible damage to the cell.[1] These phase transitions can result in changes to the fluidity of the lipid hydrocarbon tails (*e.g.* the fluid–gel transition), or cause the rearrangement of the lipids from a fluid lamellar (L_α) bilayer structure into non-bilayer structures such as the inverse hexagonal (H_{II}) phase. The H_{II} phase (Fig. 1), which consists of lipid head groups surrounding cylindrical water cores, arranged on a two-dimensional hexagonal lattice, is potentially lethal to cells as it cannot provide the semi-permeable barrier critical to cell function. This phase exists in a wide range of model lipid systems[2,3] and is particularly prevalent in systems of dioleoylphosphatidylethanolamine (DOPE).[4–6]

Pure PE membranes do not exist in nature. However, lipid species are not distributed evenly throughout cell membranes—for example in healthy mammalian cells, PE tends to concentrate in the inner membrane leaflet.[7] In addition, dehydration or temperature stress can cause lipid redistributions or phase separations.[8,9] Thus regions within membranes can become concentrated in non-bilayer forming lipids, leading to deleterious phase changes.

Some organisms and organelles have developed defences against dehydration damage, one of which is the accumulation of sugars, which have been shown to have cryoprotective properties in these systems.[10,11] The effects of sugars on the fluid–gel transition have been widely studied, and the mechanisms of protection are now reasonably well understood.[12] However, the effects of sugars on transitions to non-bilayer phases have been less well studied. Interestingly, and somewhat counter to their cryprotective nature, sugars have been shown to increase the propensity of a fully hydrated DOPE system to form the H_{II} phase at the expense of the L_α phase, in some cases completely suppressing the formation of the L_α phase.[13,14] Above a limiting hydration (known as full hydration), excess water is excluded from lipid mesophases into coexisting aqueous phases.[6] It has been established in lamellar systems that sugars are unequally partitioned between the membrane and excluded phases.[15–17] Therefore, to fully understand the mechanisms by which sugars affect the

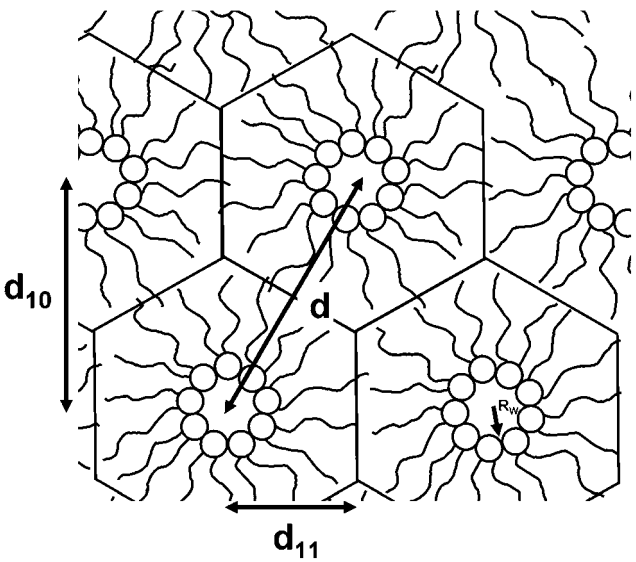

Fig. 1 Schematic diagram of the H_{II} phase.

[a]*Applied Physics, RMIT University, Melbourne, Australia. E-mail: gary.bryant@rmit.edu.au; Fax: +61 3 9925 5290; Tel: +61 3 9925 2139*
[b]*National Deuteration Facility, ANSTO, Menai, Australia*
[c]*Division of Plant Sciences, Research School of Biology, The Australian National University, Canberra, Australia*
[d]*Institut Laue-Langevin, Grenoble, France*
[e]*NIST Center for Neutron Research, Gaithersburg, Maryland, USA*
[f]*GKSS Research Centre, Geesthacht, Germany*

† Electronic supplementary information (ESI) available: Differential scanning calorimetry traces. See DOI: 10.1039/b919086d

phase behaviour of H_{II} forming lipid systems, it is necessary to determine the partitioning of the sugar between the H_{II} cores and the excluded phase.

The complexity of natural biological membranes, which comprise many lipid species (as well as proteins) makes the elucidation of specific effects difficult. Here we choose to use a model system, DOPE, as its PE head group and unsaturated acyl chains are prevalent among lipids in natural membranes. This lipid also readily self-assembles into the inverse hexagonal phase over a wide temperature range. To study the effects of the sugars we choose a ratio of 0.5 glucose molecules per lipid, which is sufficiently high to affect the phase behaviour, but not high enough to introduce the complication of glass formation.[18]

In this paper, we employ small angle X-ray scattering to assign a lipid phase and combine this observation with an analysis of contrast variation small angle neutron scattering[15] to quantitatively determine the partitioning of glucose in a DOPE–water–glucose system between a fully hydrated H_{II} lipid phase and the coexisting excluded phase.

Materials and methods

DOPE was obtained from Avanti Polar Lipids and Sigma Aldrich and used without further purification. Deuterated D-glucose-d_7 was obtained from Sigma Aldrich. Two sample compositions were studied—DOPE fully hydrated in water and DOPE fully hydrated in a water–glucose solution with a lipid–glucose molar ratio 1 : 0.5. The lipid volume fraction of each sample was 0.5. Dry DOPE was measured by weight with water and glucose solution added volumetrically to each sample to achieve the desired lipid volume fraction and glucose ratio. Samples were mixed by a combination of vortex mixing with repeated temperature cycling through the L_β/L_α–H_{II} phase transitions. Sample mixing was assessed both visually and by the observation of the reproducibility of measurements (see below).

Small angle X-ray scattering (SAXS) experiments were performed on a Bruker Nanostar covering the q-range 0.035 to 0.85 Å^{-1}. Samples were transferred to aluminium samples holders with windows of 3 M clear adhesive tape, which provides very low intensity uniform background scattering. Temperature control was achieved using a circulating water chiller/heater. Samples were equilibrated for at least 15 min prior to each measurement. Exposure times were 2 h. Longer measurements were made at 25 °C on samples in 2 mm quartz capillaries (Wolfgang Muller Glas Technik, Berlin) sealed using Araldite epoxy resin. Samples were returned to their initial measurement temperature and re-measured following each measurement program to check for lipid degradation or radiation damage. No evidence of damage was found, and all measurements were found to be consistent. Additionally, measurements using the aluminium sample holder were consistent with those using the capillaries.

Preliminary SANS measurements were performed on the SANS-1 instrument at the Geesthacht Neutron Facility (Geesthacht, Germany). Final SANS measurements were conducted on the NIST Center for Neutron Research NG7 SANS instrument (Gaithersburg, Maryland). Data were collected on a 2D detector at sample to detector distances of 1 m, 4.5 m and 13.5 m,

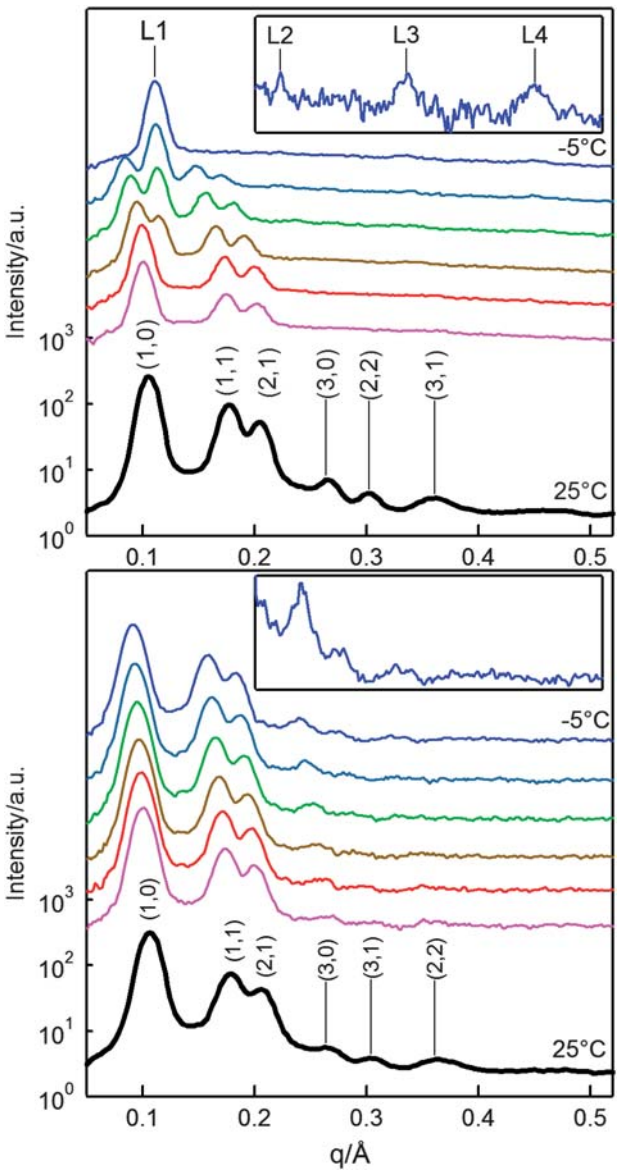

Fig. 2 SAXS measurements for the lipid–water system (top) and the lipid–water–glucose system (bottom). Temperature increases from top to bottom in 5 °C steps. Bragg reflection indices of H_{II} phase are shown in brackets. The insets show the −5 °C data on an expanded linear vertical scale.

giving a combined q-range of 3.685×10^{-3} to 0.3 Å^{-1}. Each sample composition was prepared at five D_2O–H_2O ratios: 0, 20, 40, 60 and 80% D_2O. Samples were mounted in quartz demountable cells (Hellma, Germany, 106QS, path length 0.2 mm). These cells were mounted inside titanium demountable cell holders with quartz windows and sealed with viton o-rings. The temperature of the samples was kept constant at 25 °C using a Julabo (Julabo Labortechnik Seelbach, Germany) circulating bath filled with silicon oil. Data were normalised to sample transmission, corrected for background, empty cell scattering and detector efficiency.[30] A flat incoherent scattering component determined from the scattering intensity at high q was subtracted from the data.

Results and discussion

SAXS results

Fig. 2 shows the scattering of the DOPE and DOPE–glucose samples in the temperature range −5 to 25 °C. The phase of the lipid was identified from the characteristic spacing of the higher order Bragg reflections. The lamellar L_α phase peaks index to $q_n = nq_1$ while the H_{II} phase indexes according to:

$$q_{hk} = \sqrt{(h^2 + hk + k^2)} \quad (1)$$

Up to six peaks were visible in the longer SAXS measurements, with generally only the first three peaks visible in the short runs. The H_{II}–L_α phase transition was observed in the DOPE–water sample on cooling, with a coexistence region of the two phases between −5 and 10 °C. With the addition of glucose, this transition was completely suppressed, with H_{II} observed over the accessible temperature range. The lamellar phase is identified as the fluid lamellar L_α phase. While the q-range does not extend to the wide angle region where examination of the intra-lipid peak would enable the direct determination of the degree of lipid chain fluidity, the transition temperature and d spacing of the phase (55 Å) both indicate the L_α phase. This was confirmed by differential scanning calorimetry (in ESI†) which showed a transition peak with the characteristics of a H_{II}–L_α phase transition.

Electron density profiles were reconstructed for each system at 25 °C using Fourier analysis of the SAXS data.[19] The amplitude of each Bragg peak was found by calculating the area of a fitted Gaussian curve to the background subtracted SAXS peak. Each amplitude was corrected for the multiplicity factor of the peak. A Lorentz correction was applied by dividing the peak intensity by the magnitude of the reciprocal lattice vector. Finally the amplitudes were normalised to the amplitude of the (1,0) peak. The phase of each amplitude, reduced to either positive or negative due to the centro-symmetry of the H_{II} cell, was + − − + + + as determined by Harper *et al.*[19] This has consistently been the phasing of choice for the H_{II} lipid phase, and gave the most physical result for both systems studied here. The electron density profiles determined for each system using this phasing are shown in Fig. 3. They are essentially identical, the presence of glucose slightly reducing the d spacing from 74.0 Å to 73.8 Å (note that regardless of which phasing was chosen, the two profiles were identical).

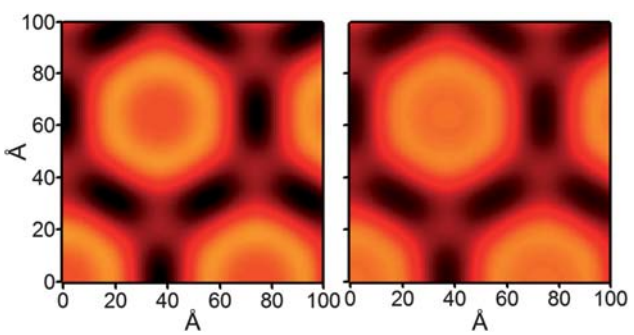

Fig. 3 Electron density profiles of the two systems studied. Lipid–water (left) and lipid–glucose–water (right).

The position of maximum electron density relative to the centre of the water core (ρ_{max}) (otherwise known as the Luzzati boundary[20]) was found to be the same for both systems within the errors: 19 ± 0.5 Å. The radius of the water core (R_w) can be determined from this value with varying degrees of accuracy depending on the number of SAXS peaks observed and their resolution. Limited resolution systematically causes ρ_{max} to be lower than R_w.[21,22] Gravimetric measurements by Tate *et al.*[6] of the DOPE–water system found the radius of the water core in fully hydrated DOPE H_{II} systems to be 21 Å at 25 °C.[6] Given the similarities in the electron densities of the systems in this study, it is reasonable to assume this value is also applicable to the lipid–water–glucose system.

The radius of the water core indicates that the volume fraction of the lipid in the H_{II} phase is $\psi_L = 0.709$. Thus it is clear that not all of the solvent in each of the systems is being incorporated into the H_{II} phase and a coexisting phase of excluded solvent exists in equilibrium with the H_{II} phase, with the volume fraction of the H_{II} and excluded phases being 0.71 and 0.29, respectively.

SANS results

The method of using contrast variation SANS to determine the partitioning of a solute between microphases in lipid systems was originally demonstrated by Demé and Zemb.[15] Briefly, two sample sets are studied—one with and one without the solute present. The contrast of the solvent (water) is varied by changing its D_2O–H_2O ratio, and the point at which the contrast of the solvent is equal to the contrast of the rest of the sample is identified—this is called the contrast match point (CMP). Considering a fully hydrated lipid H_{II} phase in a glucose–water solution, at the CMP the sum of the scattering from the membrane phase (lipid and the water and glucose in the H_{II} cores) matches the total scattering from the excess glucose–water excluded phase. Therefore at the CMP the sum of the scattering length densities (SLDs) of each of the components in the two microphases, weighted by their volume fractions, must be equal:

$$\rho_L\psi_L + \rho_S\psi_S + \rho_W\psi_W = \rho_S\psi'_S + \rho_W\psi'_W \quad (2)$$

where: ρ_L, ρ_S, and ρ_W are the scattering length densities of the lipid, solute (glucose) and water, respectively; ψ_L, ψ_S, and ψ_W are the volume fractions in the lipid phase; and ψ'_S, ψ'_W are the solute and water volume fractions in the excluded phase; and the sum of the volume fractions in each phase must be unity:

$$\begin{aligned} \psi_L + \psi_S + \psi_W &= 1 \\ \psi'_S + \psi'_W &= 1 \end{aligned} \quad (3)$$

For a three-component system consisting of lipid, glucose and water, the global volume fraction of each component is related to the local volume fractions in each phase by the following relationships:

$$\begin{aligned} \Phi_L &= \psi_L\nu \\ \Phi_W &= \psi_W\nu + \psi'_W(1-\nu) \\ \Phi_S &= \psi_S\nu + \psi'_S(1-\nu) \\ \Phi_L + \Phi_S + \Phi_W &= 1 \end{aligned} \quad (4)$$

where ν is the volume fraction of the H_{II} lipid phase relative to the total sample.

The SANS scattering results for the lipid–water and lipid–water–glucose systems are shown in Fig. 4 on double logarithmic plots. Similar SANS curves are observed for both systems, with a change in the contrast match point (*i.e.* the minimum scattering occurs at a different D_2O–H_2O ratio). The peak at high q corresponds to the main Bragg reflection observed in the SAXS experiments. The aim of contrast variation is to obtain the average scattering length density of the lipid phase. In classical contrast variation this is done by plotting $[I(0)]^{1/2}$ *vs.* contrast and determining the "match point" at which $[I(0)]^{1/2} = 0$.[23] Due to the large size of the aggregates in the hexagonal phase we cannot measure $I(0)$ directly. However, a similar analysis can be conducted by plotting $[I(q)]^{1/2}$ *vs.* contrast, which is valid as long as the match point is independent of q.[15]

To extract the contrast match point, the square root of the intensity is plotted against the D_2O–H_2O ratio for several values of q in the small angle region ($q < 0.01$ Å^{-1}), as shown in Fig. 5. In both cases the contrast match points are independent of q, negating the need to extrapolate to $I(0)$. This yields values for the CMP of $\Phi_{D_2O} = 0.198$ and $\Phi_{D_2O} = 0.092$ for the lipid–water and lipid–water–glucose samples, respectively. Using the known SLDs for D_2O and H_2O, this gives SLDs of 8.16×10^{-7} Å^{-2} and 7.94×10^{-8} Å^{-2}, respectively. These, along with the other quantities used in the analysis, are summarised in Table 1.

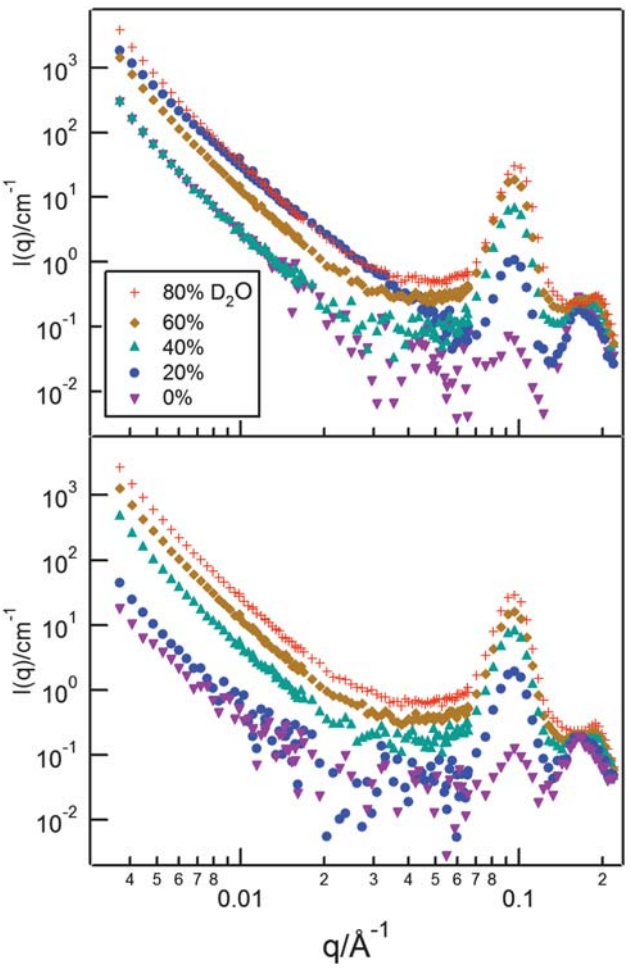

Fig. 4 SANS curves of lipid–water (top) and lipid–water–glucose (bottom) for different D_2O–H_2O ratios. The measurement of the 20% D_2O lipid–water sample was inconsistent with other measurements and was disregarded in the analysis.

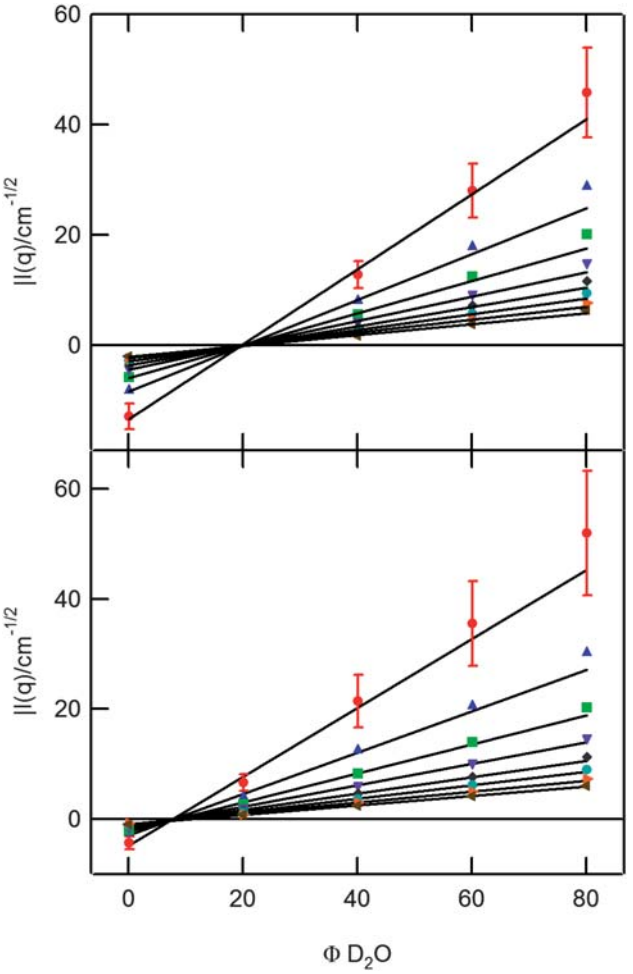

Fig. 5 Square root of intensity *vs.* volume fraction of D_2O for several values of q in the small angle region. Shown are every second curve for q values from $q = 3.685 \times 10^{-3}$ Å^{-1} to $q = 0.01$ Å^{-1}. The q independent contrast match points can be clearly seen for the lipid–water system (top) and the lipid–water–glucose system (bottom). Error bars are shown for $q = 3.685 \times 10^{-3}$ Å^{-1}.

For glucose-d_7 equilibrated in a solution with $\Phi_{D_2O} = 0.092$ the SLD is 5.74×10^{-6} Å^{-2}.[24] Solving for the local sugar volume fractions reveals $\psi_S = 0.0128$ and $\psi'_S = 0.105$. From these local volume fractions the concentration of glucose in the excess solvent phase is found to be $c' = 0.105$ (by volume), where:

$$c' = \frac{\psi'_S}{\psi'_S + \psi'_W} \quad (5)$$

This is more than twice the concentration $c = 0.044$ in the aqueous channels in the H_{II} phase and is in line with previous studies which show partial exclusion of sugars from lipid lamellar phases.[15–17,25–27] The partition coefficient of $c/c' = 0.42$ is similar to the value of 0.5 found for DMPC bilayers.[17]

Clearly these results show that the glucose is partially excluded from the water channels in the H_{II} phase. The concentration

Table 1 Quantities used in or calculated from the analysis. All quantities are dimensionless unless indicated

Quantity	Lipid–water–glucose system	Lipid–water system	Comment
Φ_L	0.5	0.5	Sample prep.
Φ_S	0.04	—	Sample prep.
Φ_W	0.46	0.5	Sample prep.
CMP	0.092	0.198	Fig. 5
SLD at CMP	7.94×10^{-8} Å^{-2}	8.16×10^{-7} Å^{-2}	Fig. 5
ψ_L	0.709	0.709	Ref. 6
ψ_S	0.0128	—	
ψ_W	0.278	0.291	
ψ'_S	0.105	—	
ψ'_W	0.895	1	
v	0.71	0.71	
n_w/n_l	15.9	16.65	
n_s/n_l	0.12	—	
c	0.044	—	
c'	0.105	—	
V_{DOPE}	1217.3 Å^3		
V_{H_2O}	30 Å^3		
$V_{glucose}$	186.5 Å^3		Ref. 28

remaining in the lipid phase corresponds to 0.12 glucose molecules per lipid (or 8.5 lipids per glucose molecule).

Studies of lamellar phases formed by phosphatidylcholine (PC) lipid model systems show that sugars are excluded from the region near the lipid–water interface[15,17,27] (the hydration layer). While the results here do not provide direct evidence, the similarity of the glucose partitioning between the DOPE system studied here and the PC systems in the literature strongly suggests that a hydration layer also exists in this system. In the case of the H_{II} phase, this would imply that the glucose molecules are in the centre of the core (on average). Thus it is unlikely that the change in the phase behaviour of the DOPE–water system due to the presence of the glucose can be attributed to direct interaction between the glucose molecules and the lipid polar head groups. Assuming the concentration of sugar at the centre of the water core is the same as the concentration of the sugar in the aqueous phase, and knowing the H_{II} geometry, the depth of the hydration layer can be estimated. In this scenario, the overall sugar concentration in the H_{II} phase ($c = 0.044$) is split into a hydration layer of pure water adjacent to the lipid head groups of depth ~7.4 Å and a cylinder of radius ~13.6 Å of sugar solution along the centre axis of the H_{II} water channel with a sugar concentration $c = 0.105$. While in reality, no such discontinuity in concentration exists, it is apparent from the size of the glucose molecules $r_g = 3.5$ Å (approximating as a sphere) that this hydration layer depth is plausible. Knowing the area per lipid at the lipid–water interface (48 Å^2, ref. 6) there are about 9.8 water molecules in the hydration layer per lipid.

The existence of the hydration layer therefore restricts the concentration of sugar in the H_{II} phase relative to the excess solvent. This difference creates an osmotic force which acts to remove water from the phase due to the difference in osmotic pressure of the solvents in the H_{II} phase and the excess solvent phase. Increasing the overall sugar concentration in the system would therefore be expected to create a larger osmotic difference between the H_{II} phase and the excess solvent and reduce the d spacing of the H_{II} phase. While the osmotic pressure difference in the systems studied here is too small to have an effect on the structural parameters of the H_{II} phase (1.05 MPa in the H_{II} phase and 2.74 MPa in the excess solution[28]), Tenchov *et al.* demonstrated this dehydrative behaviour in DHPE–water–sucrose systems.[29]

Conclusions

The results show that the addition of glucose to a fully hydrated DOPE H_{II} phase has no effect on the structure of the phase. Glucose is incorporated into the phase albeit at a lower concentration than in the surrounding excess solvent. This exclusion is consistent with the existence of a hydration layer of pure water adjacent to the lipid head groups in the H_{II} phase from which the glucose molecules are excluded, thus indicating a preference for the lipid head groups to associate with water over glucose molecules.

A consequence of the glucose concentration imbalance is the existence of an osmotic gradient between the H_{II} phase and the excess solvent which acts to remove water from the phase and favours the non-lamellar H_{II} phase over the lamellar L_α phase, due to its smaller area per lipid at the lipid–water boundary. This is evident in the thermotropic behaviour of the DOPE–water–glucose system which favours the H_{II} phase over the fluid lamellar L_α phase over a wider range of temperatures than an equivalent system without glucose.

These results highlight the complexity of the elucidation of the mechanisms with which sugars act as protectants against dehydration in natural organisms. Dehydration induced transitions such as the L_α–H_{II} bilayer to non-bilayer transition can destroy the semi-permeability of the cell membrane and are thus potentially lethal to cells. So the preference of the glucose system for the formation of the H_{II} phase over the bilayer L_α phase sits in contrast with the observed ability of sugars to prevent damage to biological cells during dehydration.

The preference for the H_{II} phase occurs in spite of the fact that most of the sugar is excluded from the H_{II} phase in a manner which suggests no direct involvement between the sugar and the lipids. Instead, with the hydration layer of pure water separating the lipid head groups from the sugar molecules, non-specific properties of the sugar such as volumetric and osmotic effects during dehydration seem to be of greater significance.

Acknowledgements

The authors are grateful for access to the major research facilities program for travel support. The access to major research facilities program is supported by the Commonwealth of Australia under the International Science Linkages program. B. Kent is the recipient of an AINSE Post Graduate Research Award. We acknowledge the support of the National Institute of Standards and Technology, U.S. Department of Commerce, in providing the neutron research facilities used in this work.

Disclaimer: Certain commercial equipment, instruments, or materials are identified in this paper to foster understanding. Such identification does not imply recommendation or endorsement by the National Institute of Standards and Technology, nor does it imply that the materials or equipment identified are necessarily the best available for the purpose.

Notes and references

1 J. Wolfe and G. Bryant, in *NATO ASI Series, Mechanics of Swelling*, ed. T. K. Karalis, Springer-Verlag, Berlin Heidelberg, 1992, vol. H 64.
2 J. M. Seddon, *Biochim. Biophys. Acta, Rev. Biomembr.*, 1990, **1031**, 1–69.
3 M. S. Webb, H. Sek Wen and P. L. Steponkus, *Biochim. Biophys. Acta, Biomembr.*, 1993, **1145**, 93–104.
4 S. M. Gruner, M. W. Tate, G. L. Kirk, P. T. C. So, D. C. Turner and D. T. Keane, *Biochemistry*, 1988, **27**, 2853–2866.
5 E. Y. Shalaev and P. L. Steponkus, *Biochim. Biophys. Acta, Biomembr.*, 1999, **1419**, 229–247.
6 M. W. Tate and S. M. Gruner, *Biochemistry*, 1989, **28**, 4245–4253.
7 P. F. Devaux, I. Lopez-Montero and S. Bryde, *Chem. Phys. Lipids*, 2006, **141**, 119–132.
8 G. Bryant, J. M. Pope and J. Wolfe, *Eur. Biophys. J.*, 1992, **21**, 223–232.
9 G. Bryant and J. Wolfe, *Eur Biophys. J. Biophys. Lett.*, 1989, **16**, 369–374.
10 J. H. Crowe, L. M. Crowe and D. Chapman, *Science*, 1984, **223**, 701–703.
11 S. Calderon, M. Holmstrup, P. Westh and J. Overgaard, *J. Exp. Biol.*, 2009, **212**, 859–866.
12 T. Lenné, G. Bryant, R. Holcomb and K. L. Koster, *Biochim. Biophys. Acta, Biomembr.*, 2007, **1768**, 1019–1022.
13 R. D. Koynova, B. G. Tenchov and P. J. Quinn, *Biochim. Biophys. Acta*, 1989, **980**, 377–380.
14 C. A. Wistrom, R. P. Rand, L. M. Growe, B. J. Spargo and J. H. Crowe, *Biochim. Biophys. Acta, Biomembr.*, 1989, **984**, 238–242.
15 B. Demé and T. Zemb, *J. Appl. Crystallogr.*, 2000, **33**, 569–573.
16 T. Lenné, G. Bryant, C. J. Garvey, U. Keiderling and K. L. Koster, *Z. Phys. B: Condens. Matter*, 2006, **385–386**, 862–864.
17 P. Westh, *Phys. Chem. Chem. Phys.*, 2008, **10**, 4110–4112.
18 J. Wolfe and G. Bryant, *Cryobiology*, 1999, **39**, 103–129.
19 P. E. Harper, D. A. Mannock, R. N. A. H. Lewis, R. N. McElhaney and S. M. Gruner, *Biophys. J.*, 2001, **81**, 2693–2706.
20 V. Luzzati, in *Biological Membranes: Physical Fact and Function*, ed. D. Chapman, Academic Press, London, 1968, vol. 1, pp. 71–123.
21 M. Rappolt, A. Hickel, F. Bringezu and K. Lohner, *Biophys. J.*, 2003, **84**, 3111–3122.
22 D. C. Turner and S. M. Gruner, *Biochemistry*, 1992, **31**, 1340–1355.
23 H. B. Stuhrmann and R. G. Kirste, *Z. Phys. Chem.*, 1967, **56**, 334–341.
24 V. F. Sears, *Neutron News*, 1992, **3**, 26–37.
25 G. Bryant and K. L. Koster, *Colloids Surf., B: Biointerfaces*, 2004, **35**, 73–79.
26 K. L. Koster, K. J. Maddocks and G. Bryant, *Eur. Biophys. J.*, 2003, **32**, 96–105.
27 F. Pincet, E. Perez and J. Wolfe, *Cryobiology*, 1994, **31**, 531–539.
28 K. Kiyosawa, *Bull. Chem. Soc. Jpn.*, 1988, **61**, 633–642.
29 B. Tenchov, M. Rappolt, R. Koynova and G. Rapp, *Biochim. Biophys. Acta, Biomembr.*, 1996, **1285**, 109–122.
30 S. R. Kline, *J. Appl. Crystallogr.*, 2006, **39**, 895–900.

